Reclamation of backwash water by cross flow microfiltration- a case study

M. T. Hung and J. C. Liu

ABSTRACT

Cross flow microfiltration (MF) for reclaiming backwash water from two water treatment plants was studied. The results showed that both transmembrane pressure (TMP) and cross flow velocity affected the permeability significantly. Cake resistance (R_c) contributed to the majority of total filtration resistance among all MF experiments. It was found that higher solid loading of backwash water did not lead to lower permeability. On the contrary, size distribution and fractal dimension of particulate matters in backwash water were more important in determining specific cake resistance and permeability. Packing of particulate matters with higher fractal dimension induced more compact structure of cake layer, which resulted in higher specific cake resistance. It was found that the effect of fractal dimension on cake compressibility was insignificant, probably because of the decrease in cake deposition during turbulent cross flow MF. Theoretical analysis on the size distribution of deposited particulate matters indicated that the proportion of submicron to micron particulate matters deposited became higher when cross flow velocity was increased. As a result, cake porosity became lower when under turbulent cross flow. Permeate quality was satisfactory in meeting drinking water standards.

Key words | backwash water, cake structure, cross flow, microfiltration, reclamation

M. T. Hung
J. C. Liu (corresponding author)
Department of Chemical Engineering,
National Taiwan University of Science and Technology,
43, Keelung Road, Section 4, Taipei106,
Taiwan
Tel.: 886-2-2737-6627
E-mail: *liu@ch.ntust.edu.tw*

NOMENCLATURE

A_1	the empirical coefficient in Equation (6)
C_b	particle concentration in bulk solution on volume ratio
C	particle wall concentration on volume ratio
D_B	the diffusivity of particle (m^2/s)
D_s	the induced diffusivity of particle (m^2/s)
d	equivalent diameter of filter channel (m)
g	the standard acceleration of gravity (m/s^2)
k_B	the Boltzmann constant (J/K)
L	the membrane length (m)
l	the channel height (m)
m	cake mass per unit of filtration area (kg/m^2)
n	cake compressibility
R_c	cake resistance (1/m)
$R_{m,b}$	resistance of blank membrane (1/m)
$R_{m,f}$	resistance of fouled membrane without cake (1/m)
R_t	total filtration resistance (1/m)
r_p	radius of particle (m)
T	the ambient temperature (°C)
U_m	the maximum flow velocity at channel entrance (m/s)
V_s	volume of particle in cake (m^3)
V_w	volume of moisture in cake (m^3)
v	cross flow velocity (m/s)
v_b	the Brownian diffusion velocity (m/s)
v_g	the gravitational settling velocity (m/s)
v_l	the lateral inertial lift velocity (m/s)
v_s	the effective back transport velocity by shear induced migration (m/s)
W_{dry}	mass of dry cake per unit of filtration area (kg/m^2)

doi: 10.2166/aqua.2007.025

W_{wet} mass of wet cake per unit of filtration area (kg/m^2)

GREEK LETTERS

α_{av} average specific cake resistance (m/kg)
$\Delta\rho$ the effective density of particle in medium (kg/m^3)
ΔP transmembrane pressure (kPa)
γ_w the shear rate on the membrane surface (1/s)
ρ_s particle density (kg/m^3)
ρ_w fluid density (kg/m^3)
μ fluid viscosity (Pa's)
υ the kinematic viscosity of dispersed medium (m^2/s)
τ the shear stress (kg/m)

INTRODUCTION

Rapid sand filters in water treatment plants need to be backwashed routinely. Consequently, a considerable amount of the produced water is required to conduct backwash process, which approximately consumes 2–5% of total water production in the water treatment plant (Cornwell & MacPhee 2001). Contaminants in raw water, such as inorganic and organic particulates, microorganisms, and dissolved organic matters captured during filtration are present in backwash water (Adin *et al.* 2002). Significant increase in contaminant concentrations has been indicated. As a result, there is increasing demand for sound management of the backwash water for either discharge or recycle. Significant numbers of waterworks in the US recycle and reuse backwash water (Arora *et al.* 2001). The coagulation-flocculation with alum has been indicated to effectively remove turbidity and *Cryptosporidium* by 93% as well as Coxsackie's A9 by 73% (Adin *et al.* 2002). Edzwald & Tobiason (2002) have shown that dissolved air flotation (DAF) is effective in removal of oocysts from the influent with recycled backwash water. Although these technologies can remove most of the pathogens from backwash water, the required secure retention of microorganisms cannot cost effectively be guaranteed (Brügger *et al.* 2001). The discussion of reusing the backwash water today often results in considering the use of membrane technology (Lipp *et al.* 1998). Jacangelo *et al.* (1995) conducted microfiltration (MF) and ultrafiltration (UF) to remove *Cryptosporidium*, *Giardia*, and MS2 virus from sample water. Their results indicate that no cysts and oocysts are detected in the permeate as long as membrane remains intact during filtration. Vigneswaran *et al.* (1996) conducted cross flow microfiltration (MF) with backflush to recover backwash water. Their experimental data reveal that cross flow MF is technically feasible and highly efficient for backwash water treatment. Full-scale recovery of backwash water by dead-end ultrafiltration (UF) has been shown to be energy efficient and very stable (Willemse & Brekvoort 1999). It has been observed that backwash water can be directly pumped into MF equipped with appropriate membrane and the permeate quality can meet EU drinking water standards without pre-settlement (Song *et al.* 2001). In their study, pre-chlorination and coagulation with the optimum polyaluminium chloride (PACl) dosage can significantly enhance the performance of downstream MF in terms of fouling reduction. Brügger *et al.* (2001) have found that UF membranes made from polyamide and polyacrylonitrile always generate permeate with good quality with low particles counts in treating backwash water. Nasser *et al.* (2002) have proposed that alum flocculation pretreatment prior to UF units enhances the removal of small particles; consequently it also reduces membrane fouling and prolongs the duration of filtration. Vos *et al.* (1997) summarize the advantages of the UF membrane technique on reuse of backwash water as excellent permeate quality, over 93% of the wastewater recovery, and no possibility of pollution from outside.

The particle size distribution of sample suspension can dramatically affect cake properties, such as porosity and specific cake resistance for cross flow filtration. The effect of particle size on the performance of cross flow microfiltration has been examined (Lu & Hwang 1995; Hwang *et al.* 2001, 2006). Their results show that the increase in transmembrane pressure (TMP) will cause the filter to have a little wider particle size distribution. Since higher filtration pressure will exert higher compressive pressure on the cake. Therefore, the cake porosity will decrease as the specific cake resistance increases with increasing filtration pressure. Furthermore, increasing cross flow velocity leads to the increase of average specific cake resistance and the decrease of cake porosity.

They have proposed that the particle packing modes are completely different for submicron and micron particles. The micron particles in a filter are in contact with each other in most conditions, and the cake porosity always increases with cross flow velocity. However, submicron particles are separate from each other because of the dominant electrostatic repulsive force. Since the double layer on the particle surface has a lubricant effect, an increase in cross flow velocity leads to a decrease in packing porosity.

In microfiltration of coagulated particles, the structure of flocs as judged by fractal dimension, dF, plays an important role in determining cake porosity and specific cake resistance. In studying polystyrene latex particles aggregated in 0.2 M NaCl solution, researchers have indicated that the dependence of cake permeability on the fractal dimension is negligible when dF value is below 2.4. However, cake porosity becomes much smaller for a fractal dimension higher than about 2.4 (Lee *et al.* 2003; Park *et al.* 2006, 2007). Cho *et al.* (2005, 2006) have investigated the effects of floc structure on permeability in the coagulation-MF process by using PACl as a coagulant. Their results depict that the flux of MF of flocs with lower fractal dimension (ca. 1.8) is higher than that of flocs with higher fractal dimension (ca. 2.0). Meng *et al.* (2005) have investigated the cake layer permeability in MF of activated sludge. Although fractal dimension of sludge slightly drops from 1.997 to 1.976, the porosity of cake layer surface is increased by almost 4 times. Generally speaking, the permeability of cake layer would increase with decreasing fractal dimension. However, Pan *et al.* (2005) have observed that the permeability of MF has nothing to do with fractal dimension and size of flocs but with the ratio of smaller particles in the suspension.

There still exist some key issues, such as the minimization of fouling, the effects of water chemistry of backwash water, and the effects of operational conditions which need to be studied regarding the use of membrane processes to reclaim backwash water. This study was conducted to determine the membrane permeability of cross flow microfiltration in reclaiming two backwash waters from water treatment plants in Taipei. The classification of specific resistances was assessed to identify the fouling mechanisms. In order to assess cake structure, size distribution and fractal dimension of particulate matters in backwash waters were measured. In addition, size distribution of particulate matters deposited on the membrane was modeled to interpret the effect of cross flow velocity on specific cake resistance.

THEORY

Generally the total filtration resistance (R_t) can be divided into three specific resistances as follows:

$$R_t = R_{m,b} + R_{m,f} + R_c \tag{1}$$

$R_{m,b}$, $R_{m,f}$, and R_c are the resistance from the blank membrane, fouling, and cake, respectively. Each specific resistance was obtained by conducting a series of filtration experiments with procedures described in our pervious work (Hung & Liu 2006).

The specific cake resistance (α_{av}) can be calculated by:

$$\alpha_{av} = \frac{R_c}{m} \tag{2}$$

m is the cake mass per unit filtration area. Furthermore, the relationships between α_{av} and the TMP can be expressed by the following empirical Equation (Tiller *et al.* 1980):

$$\alpha_{av} = A_1 \cdot \Delta P^n \tag{3}$$

A_1 is the empirical coefficient and n is the compressibility coefficient of cake.

In cross flow microfiltration, particle deposition is determined by the difference between negative forces which drive particles toward the membrane surface and positive forces which move particles away from the membrane. The negative forces include permeate drag force (F_d) and gravitational settling force (F_g), while positive forces consist of Brownian diffusion force (F_b), lateral inertial lift force (F_l) and shear induced force (F_s). The velocity corresponding to each force can be calculated by the equations as follows (Yoon *et al.* 1999):

(a) Gravitational settling velocity

$$v_g = \frac{2r_p^2 \Delta\rho g}{9\mu} \tag{4}$$

r_p is the particle radius, $\Delta\rho$ is the density difference between particles and dispersing medium, g is the gravitational acceleration, and μ is the viscosity of fluid.

(b) Brownian diffusion velocity

$$v_b = 0.807\left(\frac{D_B^2\gamma_w}{L}\right)^{1/3}\ln\left(\frac{C_w}{C_b}\right) \tag{5}$$

D_B stands for diffusivity of particle, γ_w represents the shear rate at the membrane surface, L stands for the membrane length, C_w depicts the particle wall concentration, and C_b represents the particle concentration in bulk solution. The diffusivity D_B is calculated by the Stokes-Einstein equation as:

$$D_B = \frac{k_B T}{6\pi\mu r_p} \tag{6}$$

k_B is the Boltzmann constant and T is the absolute temperature.

(c) Lateral inertial lift velocity I (only available for laminar flow condition)

$$v_l = 0.577\frac{r_p^3}{l^2}\frac{U_m^2}{\nu} \tag{7}$$

U_m is the maximum flow velocity at channel entrance, l is the channel height and ν is the kinematic viscosity of dispersing medium.

(d) Lateral inertial lift velocity II (only available for particulate matters within sublayer under turbulent flow condition) (Vasseur & Cox 1976). Basically, it was assumed that all particles subject to force analysis were very close to the membrane surface. For the calculation of inertial lift velocity of particulate matter under turbulent flow with Equation (8), that particulate matter has to be located within the sublayer (Bird *et al.* 2001). The thickness of the sublayer under turbulent flow in this study has been assessed (not shown here), which allowed particulate matters that may deposit to be fully immerged in. As a result, Equation (8) was justified to be used to calculate the inertial lift velocity in current work.

$$v_l = \left(\frac{55\gamma_w^2}{576\nu}\right)\cdot r_p^3 \tag{8}$$

(e) Shear induced diffusion velocity

$$v_s = 0.807\left(\frac{D_s^2\gamma_w}{L}\right)^{1/3}\ln\left(\frac{C_w}{C_b}\right) \tag{9}$$

D_s depicts the effective particle diffusivity, which is a function of radius of particles, r_p, and can be estimated from the equation as:

$$D_s = 0.03 r_p^2\gamma_w \tag{10}$$

If permeation drag velocity is equal to the total particle back-transport velocity, then

$$J_v = V_B(r_p) + V_l(r_p) + V_s(r_p) - V_g(r_p) \tag{11}$$

Particle with radius r_p would not move toward membrane under given flux. In other words, any particle whose radius is larger than r_p is unable to reach either membrane or cake surface since total back-transport velocity is higher than permeate drag velocity.

The shear rate (γ_w) for the cross flow membranes under given linear velocity is calculated as follows (Streeter & Wiley 1985).

Laminar flow (Re $<$ 2,000)

$$\gamma_w = \frac{\tau}{\mu} = \frac{8v}{d} \tag{12}$$

Turbulent flow (Re $>$ 2,000)

$$\gamma_w = \frac{\tau}{\mu} = 0.0395\cdot\rho^{0.75}v^{1.75}\mu^{-0.75}d^{-0.25} \tag{13}$$

τ is the shear stress, v is the cross flow velocity, d is the equivalent diameter of channel and Re is the Reynolds number.

The particle wall concentration (C_w) cannot be measured directly during filtration. Consequently, in this study, solid volume fraction of cake was designated as surrogate for C_w instead. It can be assessed as:

$$C_w = \frac{V_s}{V_s + V_w} \tag{14}$$

$$\frac{W_{\text{wet}}}{W_{\text{dry}}} = 1 + \frac{\rho_w\cdot V_w}{\rho_s\cdot V_s} = 1 + \frac{\rho_w\cdot(1 - C_w)}{\rho_s\cdot C_w} \tag{15}$$

ρ_s is the density of solid in backwash, ρ_w is the density of water, V_s is the volume of solid in cake, V_w is the volume of water in cake, W_{wet} is the weight of wet cake, and W_{dry} is the weight of dry cake.

MATERIALS AND METHODS

Backwash water was sampled from two municipal water treatment plants. One is Chang-Hsing water treatment plant (CHWTP), the biggest branch of Taipei Water Department which supplies 530,000 tons of potable water daily. The CHWTP is equipped with 24 rapid sand filters and each filter requires 10 minutes of backwashing every 24 hours. Approximately 500 tons of produced water is needed for each filter during each backwash. The backwash water from 24 filters consumes 2–3% of total water production of CHWTP. The backwash water sample was collected while 2 minutes of backwashing elapsed. The other sampling site is Swan-Sea water treatment plant (SSWTP) which supplies 23,000 tons of potable water daily. There are 8 rapid sand filters with backwash process conducted every 55 hours. Each filter needs around 280 tons of produced water for each backwashing. The backwash water accounts for 4–5% of total water production of SSWTP. The backwashing process is composed of 5-minute air scouring followed by 38-minute water flushing. Backwash water was batch-grabbed at the 3rd, 5th and 7th minute from the beginning of water flushing, and representative sample was made by mixing those batch-grabbed wastewaters.

The analytical methods for total solid (TS), total suspended solid (TSS) and dissolved organic carbon (DOC) were adopted from *Standard Methods* (APHA 1995). The pH was measured by pH meter (Orion, Model-210). The turbidity was assessed by a turbidimeter (Merck, Turbiquant 1500T). The absorbance at wavelength of 254 nm was measured utilizing a spectrophotometer (Shimadzu, UV-160A). The measurement of conductivity was accomplished with a conductivity gauge (Thermo Orion, model 105). Small-angle light scattering instrument (Malvern, Mastersizer 2000) was used to measure particle size distribution of particulate matters in backwash waters. This instrument is capable of characterizing particles with size ranging from 20 nm to 2,000 μm. Figures 1(a) and (b) show volume-based and number-based size distribution of particulate matters, respectively. The median size of particulate matter from SSWTP, 76.0 μm, is larger than that, 58.6 μm, from CHWTP. Notably, a considerable amount of submicron particulate matters were found in the backwash water from CHWTP. Fractal dimension of particulate matters was obtained from light scattering data (Lee *et al.* 2003). The zeta potential of

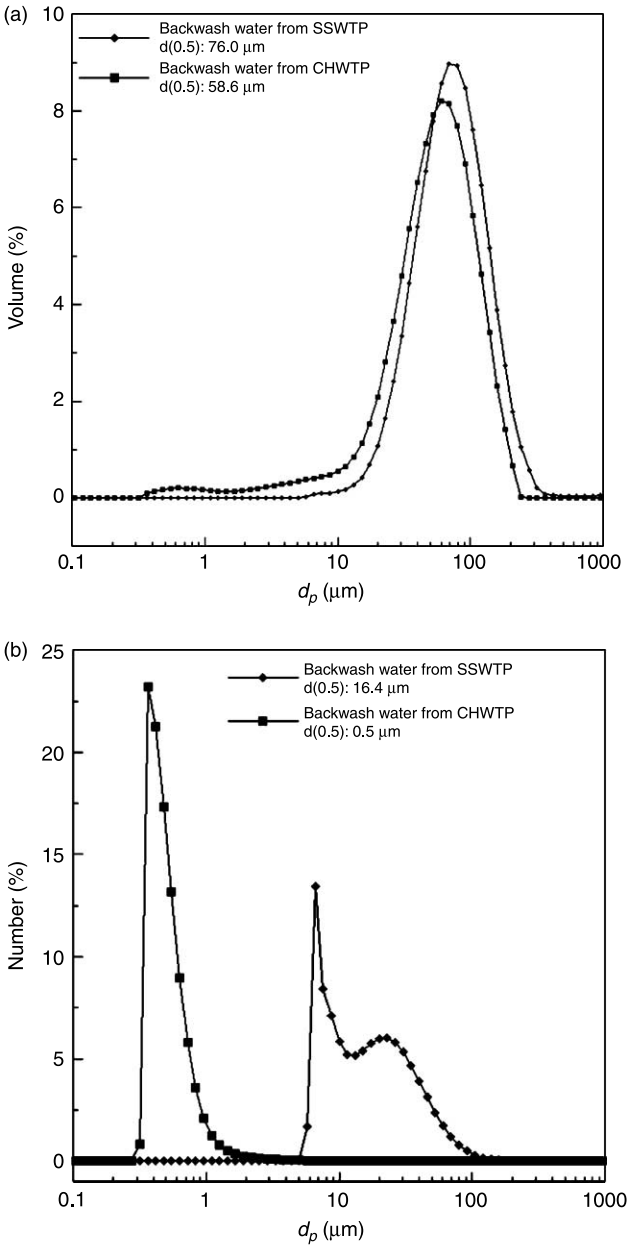

Figure 1 | (a) Volume-based size distribution of two backwash waters. (b) Number-based size distribution of two backwash waters.

particulate matters was measured by zetameter (Malvern, S2000). The true densities of solids from SSWTP and CHWTP were 2.49 g/cm^3 and 2.72 g/cm^3, respectively as measured by Schott Duran Pycnometer 24/8 (Micrometrics). Aluminum content in particulate matters from two backwash waters was assessed by adjusting the pH to 2.5 using sulfuric acid. After 2 hours of sludge acidification with continuous mixing, its supernatant was decanted and filtered with Whatman GF/C membrane. The aluminum concentration of filtrate was determined by an inductively coupled plasma atomic emission spectrometry (Perkin Elmer, ICP optima 3000). The difference on weight before and after ignition at 550 °C was the total organic content for particulate matter. The characteristics of backwash water samples from SSWTP and CHWTP are shown in Table 1.

Equipment of cross flow MF system is shown in Figure 2. A custom-made plate and sheet type module which measures 4 cm in length and 1 cm in width was used for this study. Two litres of backwash water was first placed in the suspension tank connected with a thermostatic device which kept the whole system at a constant temperature of 25°C. The peristaltic pump (Cole-Parmer, Masterflex) not only accounted for transportation of backwash water but also provided transmembrane pressure (TMP) as the driving force for MF. The rotameter (Aalborg, P11A2) prior to filter

Table 1 | Characteristics of backwash water

Parameter (unit)	SSWTP	CHWTP
pH (–)	7.08	7.11
Turbidity (NTU)	25.7	641
TS (mg/l)	154.7	797
TSS (mg/l)	91.7	748
DS (mg/l)	63	49
Zeta potential (mV)	−13.3	−9.2
UV_{254} absorbance (cm^{-1})	0.011	0.005
DOC (mg/l as C)	2.2	1.27
Conductivity (μs/cm)	139	88.2

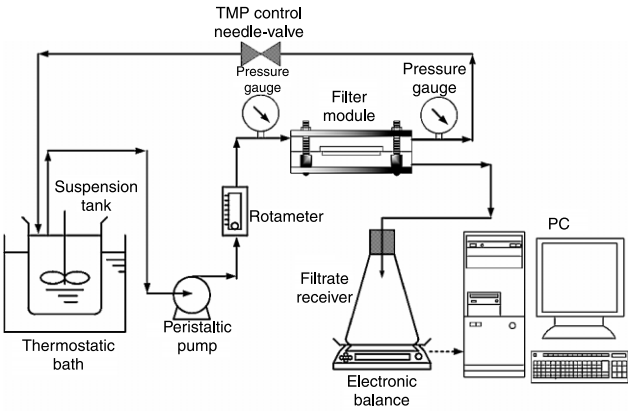

Figure 2 | Scheme of cross flow microfiltration system.

module was used to monitor cross flow velocity, which was chosen to be 0.43 and 1.11 m/s, respectively, in order to assess laminar and turbulent flow. Two pressure gauges were used to examine the TMP, which was kept at 20, 40 and 60 kPa, respectively. As the filtration experiment proceeded, filtrate flowed into the glass receiver and its weight was measured by an electronic balance (Ohaus, Adventurer). Meanwhile, a personal computer connected to the balance recorded the weight as a function of operation time. Notably, the solid loading of backwash water was monitored and kept at its initial magnitude via supplementing with produced water from water treatment plants, so that the turbidity was constant throughout. Hydrophilic mixed cellulose ester membrane (Corning, Membra-Fil) with the nominal pore size of 0.2 μm was chosen for MF. Before conducting MF, the membrane was first filtered with ultrapure water to examine the blank membrane resistance ($R_{m,b}$). After accomplishing the experiment, the membrane was taken out from the module, and the cake layer was gently removed from the used membrane, then it was reserved for measuring the weights of wet and dry cake. Afterwards, used membrane was used for again filtering with ultrapure water to assess the fouling resistance ($R_{m,f}$).

RESULTS AND DISCUSSION

Flux and classification of hydrodynamic resistance

Flux of cross flow microfiltration of the backwash water from SSWTP as affected by TMP under laminar and turbulent

cross flow is illustrated in Figures 3(a) and 3(b), respectively. The corresponding Reynolds number was 1,583 and 4,115, respectively under laminar and turbulent cross flow velocity conditions. When under laminar flow condition, the initial flux was 3,150, 5,040, and 7,020 l/m^2·h, respectively, under TMP of 20, 40, and 60 kPa. The flux at the end of experiment dropped to 173, 161, and 149 l/m^2·h, respectively, under TMP of 20, 40, and 60 kPa. It was found that higher TMP resulted in higher initial flux, which then decreased to even lower than that of lower TMP. It inferred that higher TMP induced higher drag force toward membrane, higher initial flux, and more rapid cake deposition. When under turbulent flow condition, the initial flux was 3,820, 5,790, and 7,900 l/m^2·h, respectively, under TMP of 20, 40, and 60 kPa. The initial flux also increased with the increase in TMP. The flux at the end of the experiment declined to 180, 187, and 184 l/m^2·h, respectively, under TMP of 20, 40, and 60 kPa. Extents of flux decline under TMP of 40 and 60 kPa were less than those under laminar cross flow. Meanwhile, fluxes at the end of MF with TMP of 40 and 60 kPa were slightly higher than that under 20 kPa. Figures 4(a) and 4(b) display flux in MF of backwash water from CHWTP. When under laminar flow condition, the initial flux was 3,080, 3,630, and 4,510 l/m^2·h, respectively, under TMP of 20, 40, and 60 kPa. The flux at the end of the experiment dropped to 370, 320, and 288 l/m^2·h, respectively, under TMP of 20, 40, and 60 kPa. When under turbulent flow condition, the initial flux was 3,840, 4,430, and 5,670 l/m^2·h, respectively, under TMP of 20, 40, and 60 kPa. The flux at the end of the experiment declined to 374, 347, and 334 l/m^2·h, respectively, under TMP of 20, 40, and 60 kPa. The TMP effect on MF permeability under two cross flow conditions was similar to

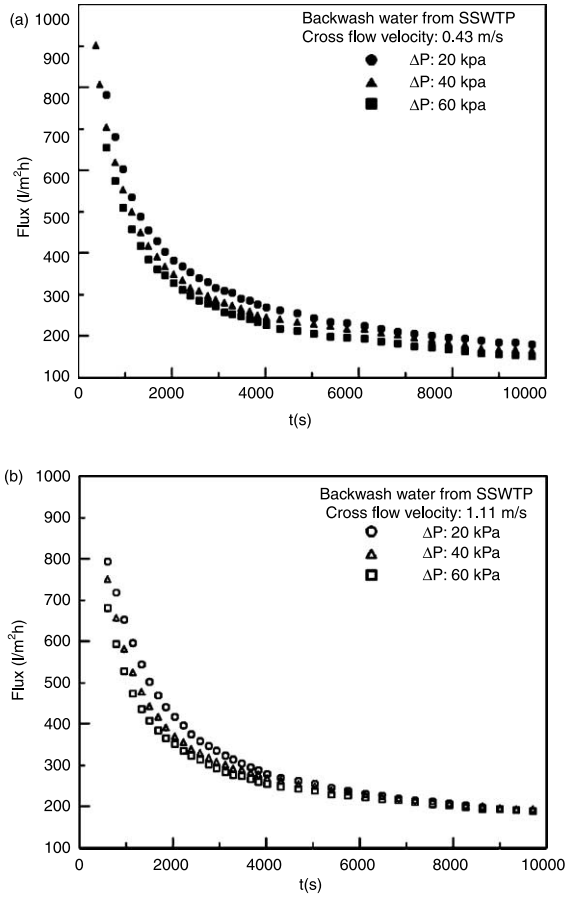

Figure 3 | (a) The flux as affected by TMP under laminar cross flow in the case of SSWTP. (b) The flux as affected by TMP under turbulent cross flow in the case of SSWTP.

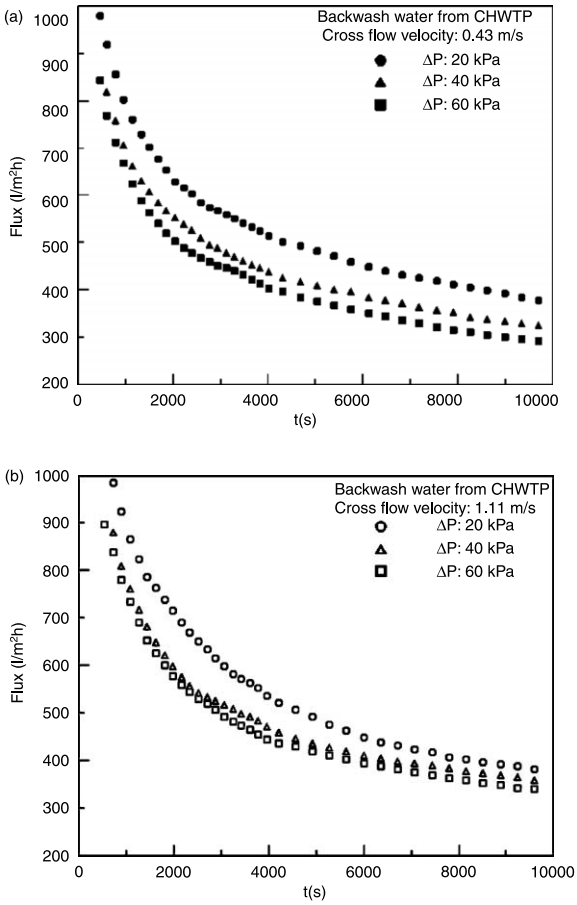

Figure 4 | (a) The flux as affected by TMP under laminar cross flow in the case of CHWTP. (b) The flux as affected by TMP under turbulent cross flow in the case of CHWTP.

the case of SSWTP. Likewise, increasing cross flow velocity from laminar to turbulent regime reduced the extent of flux decline and increased the flux in later period of MF with TMP of 40 and 60 kPa. Knowing that solid loading of backwash water from CHWTP was substantially higher than that of backwash water from SSWTP, interestingly, the permeability of MF in the case of CHWTP was all higher than that of SSWTP under comparable operational conditions.The specific resistances, including $R_{m,b}$, $R_{m,f}$, R_c and R_t, derived from MF of backwash waters from SSWTP and CHWTP are depicted in Tables 2(a) and 2(b), respectively. It is evident that both resistance from fouling ($R_{m,f}$) and blank membrane ($R_{m,b}$) contributed an insignificant portion to the total filtration resistance, and were independent of TMP in all MF experiments. It implied that adsorption of organic matters present in backwash water onto the pore wall was negligible. Furthermore, submicron particulate matters present in backwash water from CHWTP did not cause significant increase in fouling resistance. Cake resistance (R_c) was the predominant one among all resistance regardless of operational conditions. In other words, permeability of MF was profoundly influenced by cake characteristics. Table 3(a) shows key characteristics of the cake formed in MF of the backwash water from SSWTP including dry cake mass and specific cake resistance. It was found that increase in TMP led to increase in cake deposition. By increasing cross flow velocity from laminar to turbulent cross flow, cake deposition was reduced slightly by 3.6%, 8.3% and 13.7%, respectively under TMP of 20, 40 and 60 kPa. It is reasoned that higher shear stress was not effective in reducing the cake deposition. When comparing the specific cake resistances in MF under two different flow regimes, we found only an insignificant difference when at TMP of 20 kPa. Nevertheless, specific cake resistance was decreased by 7.2% and 6.4%, respectively for MF operated under TMP of 40 and 60 kPa when turbulent cross flow was applied. Compressibility coefficients in the case of SSWTP were 0.61 and 0.56, respectively under laminar and turbulent cross flow as calculated by Equation (3). Therefore, the increase in cross flow velocity slightly reduced cake compressibility, which allowed cake to form a looser structure under higher TMP as compared with a cake formed under laminar cross flow. Table 3(b) shows the cake properties in the case of CHWTP. The correlation between cake deposition and TMP was identical to the case of SSWTP. However, it was found that higher shear stress effectively limited cake formation. Nevertheless, when at identical TMP, higher specific cake resistance was found when under turbulent cross flow as compared with that under laminar cross flow. This phenomenon is further discussed in the later section when assessing size of deposited particulate matters during MF.

Cake structure and permeability

The characteristics including fractal dimension, total organic matter and total aluminum of particulate matters present in backwash waters from two water treatment plants are shown in Table 4. Fractal dimension of particulate matters in the backwash water from SSWTP (i.e. $d_F = 2.77$) was much higher than that of particulate matters in the backwash water from CHWTP (i.e. $d_F = 1.92$). The dF value of backwash water from SSWTP was considered to be unreasonably high. Lee *et al.* (2005) have revealed that the dF value in the 2.3–2.5 range or higher is possibly observed when "restructuring" of flocs occurs. Therefore, it is probably due to the fact that the particulate matters in the backwash water from SSWTP was subject to compression and consequently deformed in the course of sand filtration. In Table 4, total Al(III) concentration in the particulate matters from SSWTP was three times higher than that from CHWTP. The structure of the particulate matters in coagulation-flocculation process of SSWTP might be looser and more compressible due to higher aluminum hydroxide content (Knocke *et al.* 1987). When those unsettled particulate matters with looser structure were captured by sand filter in SSWTP, the deformation of particulate matters took place as filtration time elapsed. Notably, the backwash process of sand filters was conducted every 55 hours in SSWTP. It implies that those particulate matters underwent a longer compression period, and it might be the reason for the particulate matters from SSWTP to have such a high fractal dimension.

Lee *et al.* (2003) have investigated the effect of floc size and structure on cake resistance in dead end microfiltration and indicated that floc structure effects appear to be significant for cakes made of small flocs (i.e. 8.1–17 μm), but negligible for cakes made of large flocs (i.e. 40.6–48.5 μm). Large flocs would form a cake with large inter-

Table 2(a) | The classification of hydrodynamic resistances in the case of SSWTP

TMP (kPa)	$R_{m,b}(1/m) * 10^{10}$	$R_{m,f}$	R_c	R_t
Cross flow velocity: 0.43 m/s				
20	2.2	0.3	39.1	41.6
	(5.3%)	(0.7%)	(94.0%)	(100%)
40	2.3	0.7	86.4	89.4
	(2.6%)	(0.8%)	(96.6%)	(100%)
60	2.3	0.7	142	145
	(1.6%)	(0.4%)	(98.0%)	(100%)
Cross flow velocity: 1.11 m/s				
20	2.0	0.3	37.1	39.4
	(5.0%)	(0.8%)	(94.2%)	(100%)
40	2.0	0.6	73.5	76.1
	(2.6%)	(0.8%)	(96.6%)	(100%)
60	2.1	0.8	114	117
	(1.8%)	(0.7%)	(97.4%)	(100%)

Table 2(b) | The classification of hydrodynamic resistances in the case of CHWTP

TMP (kPa)	$R_{m,b}(1/m) * 10^{10}$	$R_{m,f}$	R_c	R_t
Cross flow velocity: 0.43 m/s				
20	1.9	0.3	17.3	19.5
	(9.7%)	(1.5%)	(88.7%)	(100%)
40	2.2	0.3	42.4	44.9
	(4.9%)	(0.7%)	(94.4%)	(100%)
60	2.6	0.3	72.1	75.0
	(3.5%)	(0.4%)	(96.1%)	(100%)
Cross flow velocity: 1.11 m/s				
20	2.4	0.7	16.2	19.3
	(12.4%)	(3.6%)	(83.9%)	(100%)
40	2.4	0.4	38.7	41.5
	(5.8%)	(1.0%)	(93.3%)	(100%)
60	2.2	0.6	61.9	64.7
	(3.4%)	(0.9%)	(95.7%)	(100%)

Table 3(a) | Characteristics of filter cake in the case of SSWTP

	SSWTP	
TMP (kPa)	**Dry cake mass (g/m^2)**	**Specific cake resistance α_{av} (m/kg)**
Cross flow velocity: 0.43 m/s		
20	8.3	4.71E + 13
40	12.0	7.20E + 13
60	15.3	9.26E + 13
Cross flow velocity: 1.11 m/s		
20	8.0	4.64E + 13
40	11.0	6.68E + 13
60	13.2	8.67E + 13

Table 3(b) | Characteristics of filter cake in the case of CHWTP

	CHWTP	
TMP (kPa)	**Dry cake mass (g/m^2)**	**Specific cake resistance α_{av} (m/kg)**
Cross flow velocity: 0.43 m/s		
20	58.8	2.94E + 12
40	81.3	5.21E + 12
60	122.3	5.90E + 12
Cross flow velocity: 1.11 m/s		
20	30.8	5.25E + 12
40	48.9	7.91E + 12
60	66.8	9.26E + 12

floc porosity which results in a significantly lower resistance than achieved for smaller flocs. Concomitantly, looser flocs (of low fractal dimension) are likely to form cakes with higher intra-porosity and lower resistance than a cake made of compact flocs of similar size. Cho *et al.* (2005) study effects of floc structure on permeability in the coagulation-MF process and indicate that fractal dimension significantly affects flux behavior when floc size is larger than 138 μm. It is the presence of aluminum hydroxide that may reduce the inter-floc porosity in cake, and the intra-floc porosity becomes more profound in determining the averaged-cake porosity. This result implies that intra-floc porosity is probably as critical as inter-floc porosity on the development of cake porosity when the cake is composed of large flocs. Consequently, it can be understood that the specific resistance of MF treating the backwash water containing

Table 4 | Characteristics of particulate matters in two backwash water

Parameter	SSWTP	CHWTP
Fractal dimension (Dimensionless)	2.77	1.92
Total organic matter content (g-organic matter/g-dry solids)	0.19	0.08
Total Al(III) content (g-Al(III)/g-dry solids)	0.14	0.05

particulate matters with low fractal dimension, CHWTP, is lower than that of particulate matters with higher fractal dimension, SSWTP. This is in agreement with previous literature (Lee *et al.* 2003; Cho *et al.* 2005). Knowing that the size of particles in the current study were all large, still it was found that fractal dimension affected specific resistance to filtration. As indicated by the aluminum contents of particulate matters in two backwash waters, a significant amount of aluminum hydroxide was present in both samples. Therefore, intra-floc porosity was conceived to play an important role in determining cake-averaged porosity and specific cake resistance of MF treating two backwash waters of this study. It is the reason why cake composed of particulate matters from SSWTP had lower cake-averaged porosity as compared with that composed of particulate matters from CHWTP.

Cake formed by flocs with lower fractal dimension should be more compressible than that formed by flocs with high fractal dimension (Lee *et al.* 2003; Cho *et al.* 2005). However, no dependence of compressibility on fractal dimension has been indicated, probably because floc strength is not taken into account (Park *et al.* 2006, 2007). Cake composed of flocs with a loose structure tends to collapse under high TMP and induces higher specific cake resistance. Compressibility coefficients of the cake formed of particulate matters in the backwash water from CHWTP were 0.65 and 0.52, respectively, under laminar and turbulent cross flow. Comparing compressibility of cakes produced in MF of two backwash waters under identical operational conditions, it was found that those values were approximately equal and the effect of fractal dimension on cake compressibility was insignificant in the present work. The correlation between cake thickness and its compressibility induced by cake collapse has been addressed before (Hamachi & Mietton-Peuchot 1999; Li *et al.* 2002; Tarabara *et al.* 2004). Cake growth proceeds by, in the early stages of fouling, producing a more porous, actively growing layer that collapses once a critical thickness is reached. In other words, a more porous layer in the cake will grow until its total thickness is large enough to produce a compressive pressure which results in the collapse (Tarabara *et al.* 2004). Consequently, cake thickness may crucially determine the compressibility of the cake formed by aggregates or flocs. Cake composed of flocs with low fractal dimension in MF conducted with cross flow mode may be less compressible as compared with that in MF with dead end mode if the cake is effectively reduced by increasing cross flow velocity. Regarding the case of CHWTP, cake deposition was reduced by 40 to 48% when cross flow velocity was increased to turbulent flow regime. As a result, cake composed of particulate matters in the backwash water from CHWTP (i.e. lower fractal dimension) may not have higher compressibility than that composed of particulate matters in the backwash water from SSWTP.

Modeling of deposition of particulate matters

In order to understand the effect of cross flow velocity on specific cake resistance in the case of CHWTP, size of particulate matters deposited in the course of MF was assessed. Particle wall concentration (C_w) is an essential parameter in the assessment of size distribution of deposited particulate matters. The surrogate of C_w was the volume fraction of solid in cake formed under given conditions, as shown in Table 5. The total back-transport velocity as a function of size of particulate matter deposited under laminar and turbulent flow condition are depicted in Figures 5(a) and 5(b), respectively. Notably, the summation of individual back-transport velocities is slightly lower than the solid line for shear-induced back-diffusion as shown in

Table 5 | C_w under various conditions of MF

TMP (kPa)	C_w (volume fraction)
Cross flow velocity: 0.43 m/s	
20	0.148
40	0.162
60	0.174
Cross flow velocity: 1.11 m/s	
20	0.167
40	0.178
60	0.185

Figure 5(a). This is because the gravitational settling velocity was relatively significant in affecting total back-transport under laminar flow condition, especially as the particle size becomes large. The cut-diameter of particulate matter, which represents the maximum size of particulate matter capable of depositing at the beginning and at the end of MF, is listed in Table 6 for MF under various operation conditions. For instance, when at the very beginning of MF at TMP of 20 kPa and under laminar cross flow, particulate matters would not deposit as long as their diameters were larger than 24.0 μm. Likewise, particulate matters whose size was greater than 5.1 μm were incapable of reaching the cake surface at the end of MF. It was found that an increase in TMP caused the cake to have a slightly broader size distribution of deposited particulate matters. This observation was consistent with results found in the work by Hwang *et al.* (2006). Table 6 also indicates that deposition of micron particulate matters became less under turbulent cross flow than that under laminar cross flow. Moreover, all submicron particulate matters kept depositing over the process of MF regardless of cross flow velocity applied. As a result, the proportion of submicron to micron particulate matters was relatively higher under turbulent cross flow. The filter cake formed by submicron particles tends to be less porous as cross flow velocity is increased (Lu & Hwang 1995; Hwang *et al.* 2006). Consequently, cake porosity is significantly influenced by the proportion of

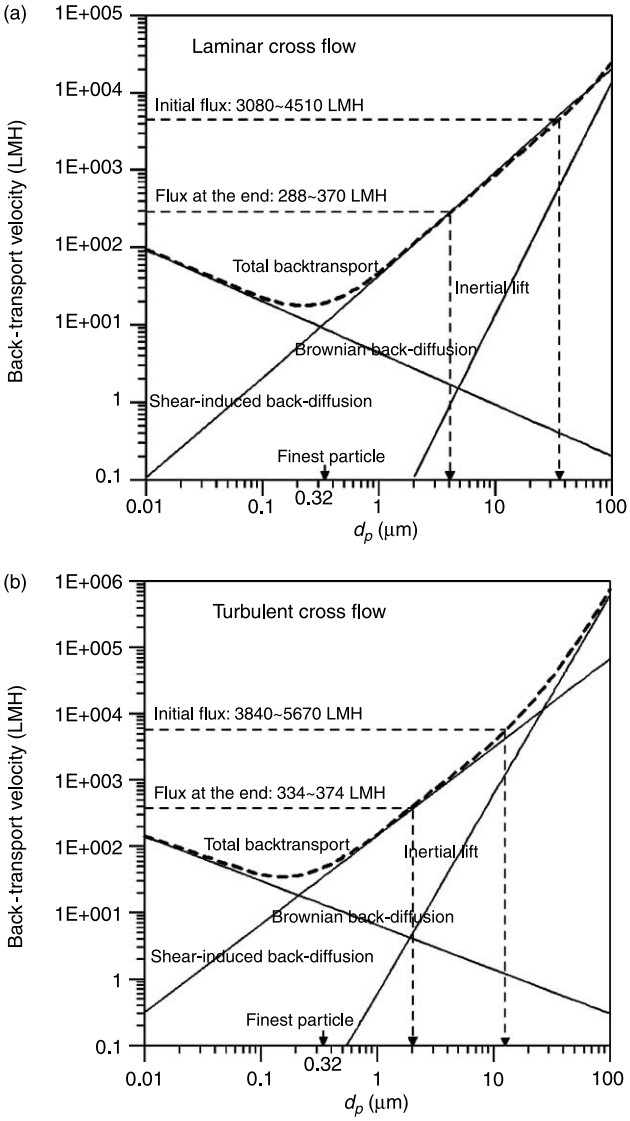

Figure 5 | (a) The total back-transport velocity as a function of size of particulate matters deposited under laminar cross flow (the gravitational settling velocity is not depicted). (b) The total back-transport velocity as a function of size of particulate matters deposited under turbulent cross flow (the gravitational settling velocity is not depicted).

submicron to micron particles deposited. A higher proportion of submicron to micron particulate matters results in a denser structure of the cake layer. It can be understood that MF of the backwash water from CHWTP produced a cake with lower porosity and simultaneously had higher specific cake resistance under turbulent cross flow. Similar phenomenon of MF has been addressed previously (Hwang *et al.* 2001). As for the backwash water from SSWTP, the

Table 6 | Cut-diameter of deposited particulate matters at the beginning and at the end of MF (Submicron particulate matters ranged from 0.32 to 0.99 μm)

	Cut-diameter of deposited particulate matter (μm)	
TMP (kPa)	At the beginning of MF	At the end of MF
Cross flow velocity: 0.43 m/s		
20	24.0	5.1
40	28.8	4.3
60	33.1	4.1
Cross flow velocity: 1.11 m/s		
20	10.1	2.0
40	11.3	1.8
60	12.6	1.6

increase in cross flow velocity results in the decrease of the specific cake resistance as indicated before (Lu *et al.* 1995). It is because all particulate matters from SSWTP were in the micron range.

Permeate water quality

Table 7 shows permeate quality from MF processes treating two backwash waters. Basically, turbidity in backwash waters was effectively removed without pretreatment. The removal of dissolved matters was limited by MF, judging by UV_{254}, DOC and conductivity of permeates. The ultra low permeate turbidity, as low as 0.04 NTU, implies that the membrane very probably remained intact during MF. Jacangelo *et al.* (1995) have indicated all tested MF membranes can remove *Giardia* cysts or *Cryptosporidium* oocysts from sampled waters as long as the membrane remains intact. As a result, cysts or oocysts might be totally rejected by the MF membrane of this study. The permeate quality could meet the drinking water standard. Therefore, reclamation of permeates for drinking water production is feasible by using cross flow MF as a treatment technique.

Table 7 | Permeate water quality

Parameter (unit)	SSWTP	CHWTP
pH (–)	6.95 ± 0.1	7.03 ± 0.07
Turbidity (NTU)	0.04 ± 0.02	0.06 ± 0.02
UV_{254} absorbance (cm^{-1})	0.011 ± 0.002	0.004 ± 0.001
DOC (mg / l as C)	1.98 ± 0.13	1.08 ± 0.05
Conductivity (μs / cm)	119 ± 1.9	84.2 ± 2.6

Regarding permeability of MF handling backwash waters from SSWTP and CHWTP, the MF experiments in the current study help to elucidate the effects of characteristics of backwash water such as solid loading (TSS), fractal dimension and size distribution of particulate matters on its permeability. Solid loading seemed relatively less important in determining permeability than other parameters. Although the increment of cake deposition might induce higher cake resistance, it was the cake structure which affected resistance more significantly. It was shown that intra-floc porosity was as important as inter-floc porosity on the development of cake porosity, which determined specific cake resistance. Consequently, fractal dimension of particulate matters in backwash water is proposed to significantly affect the specific resistance of the cake. Notably, the presence of submicron particulate matters may cause unfavorable conditions under high cross flow velocity. The proportion of submicron to micron particulate matters became higher as turbulent cross flow was implemented. As a result, the MF of backwash water with the presence of submicron particulate matters had a cake with lower porosity and higher resistance when cross flow velocity was higher. In practice, MF with constant flux mode is recommended and its initial TMP should be low to prevent serious cake compression. If cake deposition is hardly removed by shear stress exerted on the cake surface, or submicron particulate matters are present in backwash water, then an increase in cross flow velocity will not be recommended. However, further study is definitely needed on the relationships between the characteristics of backwash water and filtration behaviors, so that cost-effective strategies for MF may be formulated.

CONCLUSIONS

Solid loading of backwash water was not a major parameter in determining permeability of MF. On the contrary, size distribution and fractal dimension of particulate matters were relatively more important. Packing of particulate matters with higher fractal dimension induced a more compact structure of the cake layer, which resulted in higher specific cake resistance. The compressibility of cake composed of particulate matters with lower fractal dimension was reduced by increasing cross flow velocity because cake development was suppressed under higher shear stress. However, applying higher TMP to MF still resulted in a more rapid flux decline and lower permeability as compared with low TMP applied. The presence of submicron particulate matters in backwash water would render increasing cross flow velocity ineffective in the reduction of cake resistance. This is because deposited submicron particulate matters formed denser cake when cross flow velocity was raised, and increased specific cake resistance. Permeate quality could meet drinking water standards and reclamation of backwash water by cross flow MF was feasible. In practice, it is recommended to operate with constant flux mode and its initial TMP should be low to prevent serious cake compression. If cake deposition is hardly removed by the shear stress exerted on the cake, or submicron particulate matters are present in the backwash water, then an increase in cross flow velocity may not be effective in enhancing permeability.

REFERENCES

Adin, A., Dean, L., Bonner, F., Nasser, A. & Huberman, Z. 2002 Characterization and destabilization of spent filter backwash water particles. *Wat. Sci. Tech.: Water Supply* **2**(2), 115–122.

APHA 1995 *Standard Methods for the Examination of Water and Wastewater*, 19th edn. American Public Health Association, Washington D.C., USA.

Arora, H., Giovanni, G. D. & Lechevallier, M. 2001 Spent filter backwash water contaminants and treatment strategies. *J. AWWA* **93**(5), 100–112.

Bird, R. B., Stewart, W. E. & Lightfoot, E. N. 2001 *Transport Phenomena*. John Wiley & Sons, New York, USA.

Brügger, A., Voßenkaul, K., Melin, T., Rautenbach, R., Golling, B., Jacobs, U. & Ohlenforst, P. 2001 Reuse of spent filter backwash water by implementing ultrafiltration technology. *Wat. Sci. Tech.: Water Supply* **1**(5-6), 207–214.

Cho, M. H., Lee, C. H. & Lee, S. 2005 Influence of floc structure on membrane permeability in the coagulation-MF process. *Wat. Sci. Tech.* **51**(6–7), 143–150.

Cho, M. H., Lee, C. H. & Lee, S. 2006 Effect of flocculation conditions on membrane permeability in coagulation-microfiltration. *Desal.* **191**(1–3), 386–396.

Cornwell, D. A. & MacPhee, M. J. 2001 Effects of spent filter backwash recycle on *Cryptosporidium* removal. *J. AWWA* **93**(4), 153–162.

Edzwald, J. K. & Tobiason, J. E. 2002 Fate and removal *Cryptosporidium* in a dissolved air flotation water plant with and without recycle of waste filter backwash water. *Wat. Sci. Tech.: Water Supply* **2**(2), 85–90.

Hamachi, M. & Mietton-Peuchot, M. 1999 Experimental investigations of cake characteristics in crossflow microfiltration. *Chem. Eng. Sci.* **54**(18), 4023–4030.

Hung, M. T. & Liu, J. C. 2006 Microfiltration for separation of green algae from water. *Colloids Surfaces B* **51**(2), 157–164.

Hwang, K. J., Yu, Y. H. & Lu, W. M. 2001 Cross-flow microfiltration of submicron microbial suspension. *J. Membr. Sci.* **194**(2), 229–243.

Hwang, K. J., Hsu, Y. L. & Tung, K. L. 2006 Effect of the particle size on the performance of cross-flow microfiltration. *Adv. Powder Tech.* **17**(2), 189–206.

Jacangelo, J. G., Adham, S. S. & Laíné, J. -M. 1995 Mechanism of Cryptosporidium, Giardia, and MS2 virus removal by MF and UF. *J. AWWA* **87**(9), 107–121.

Knocke, W. R., Hamon, J. R. & Dulin, B. E. 1987 Effects of coagulation on sludge thickening and dewatering. *J. AWWA*. **79**(6), 89–98.

Lee, S. A., Fane, A. G., Amal, R. & Waite, T. D. 2003 The effect of floc size and structure on specific cake resistance and compressibility in dead-end microfiltration. *Sep. Sci. Technol.* **38**(4), 869–887.

Lee, S. A., Fane, A. G. & Waite, T. D. 2005 Impact of natural organic matter on floc size and structure effects in membrane filtration. *Environ. Sci. Technol.* **39**(17), 6477–6488.

Li, J., Yu Hallbauer-Zadorozhnaya, V., Hallbauer, D. K. & Sanderson, R. D. 2002 Cake-layer deposition, growth, and compressibility during microfiltration measured and modeled using a noninvasive ultrasonic technique. *Ind. Eng. Chem. Res.* **41**(16), 4106–4115.

Lipp, P., Baldauf, G., Schick, R., Elsenhans, K. & Stabel, H. -H. 1998 Integration of ultrafiltration to conventional drinking water treatment for a better particle removal - efficiency and costs? *Desal.* **119**(1-3), 133–142.

Lu, W. M. & Hwang, K. J. 1995 Cake formation in 2-D cross-flow filtration. *AIChE J.* **41**(6), 1443–1455.

Meng, F. G., Zhang, H. M., Li, Y. S., Zhang, X. W. & Yang, F. L. 2005 Application of fractal permeation model to investigate membrane fouling in membrane bioreactor. *J. Membr. Sci.* **262**(1-2), 107–116.

Nasser, A., Huberman, Z., Dean, L., Bonner, F. & Adin, A. 2002 Coagulation as pretreatment of SFBW for membrane filtration. *Wat. Sci. Tech.: Water Supply* **2**(5-6), 301–306.

Pan, J. R., Huang, C. P., Jiang, W. & Chen, C. H. 2005 Treatment of wastewater containing nano-scale silica particles by dead-end microfiltration: evaluation of pretreatment methods. *Desal.* **179**(1-3), 31–40.

Park, P. K., Lee, C. H. & Lee, S. 2006 Permeability of collapsed cakes formed by deposition of fractal aggregates upon membrane filtration. *Environ. Sci. Technol.* **40**(8), 2699–2705.

Park, P. K., Lee, C. H. & Lee, S. 2007 Determination of cake porosity using image analysis in a coagulation-microfiltration system. *J. Membr. Sci.* **193**(1-2), 66–72.

Song, H., Fan, X., Zhang, Y., Wang, T. & Feng, Y. 2001 Application of microfiltration for reuse of backwash water in a conventional water treatment plant - a case study. *Wat. Sci. Tech.: Water Supply* **1**(5-6), 199–206.

Streeter, V. L. & Wiley, E. B. 1985 *Fluid Mechanics*, 8th edn. McGraw-Hill, New York, USA.

Tarabara, V. V., Koyuncu, I. & Wiesner, M. R. 2004 Effect of hydrodynamics and solution ionic strength on permeate flux in cross-flow filtration: direct experimental observation of filter cake cross-sections. *J. Membr. Sci.* **241**(1), 65–78.

Tiller, F. M., Cramp, J. R. & Ville, F. 1980 In: Samasundaran, P. (ed.) *A revised approach to the theory of cake filtration*, *Fine Particles Processing*. Amer. Inst. Min. Met. Petr. Eng, New York, USA, pp. 1549–1558.

Vasseur, P. & Cox, R. G. 1976 The lateral migration of spherical particle in two dimensional shear flow. *J. Fluid Mech.* **78**(2), 385–413.

Vigneswaran, S., Boonthanon, S. & Prasanthi, H. 1996 Filter backwash water recycling using crossflow microfiltration. *Desal.* **106**(1–3), 31–38.

Vos, G., Brekvoort, Y. & Buijs, P. 1997 Full-scale treatment of filter backwash water in one step to drinking water. *Desal.* **113**(2–3), 283–284.

Willemse, R. J. N. & Brekvoort, Y. 1999 Full-scale recycling of backwash water from sand filters using dead-end membrane filtration. *Wat. Res.* **33**(15), 3379–3385.

Yoon, S. H., Lee, C. H., Kim, K. J. & Fane, A. G. 1999 Three-dimensional simulation of the deposition of multi-dispersed charged particles and prediction of resulting flux during cross-flow microfiltration. *J. Membr. Sci.* **161**(1–2), 7–20.

First received 7 November 2006; accepted in revised form 31 May 2007